DALTON
FULL PAPER

Trimethylplatinum(IV) complexes of dithiocarbamato ligands: an experimental NMR study on the barrier to C–N bond rotation

Peter J. Heard,*[a] Kenneth Kite,[b] Julie Søgaard Nielsen[a] and Derek A. Tocher[c]

[a] *School of Biological and Chemical Sciences, Birkbeck University of London, Gordon House, 29 Gordon Square, London, UK WC1H 0PP. E-mail: p.heard@chem.bbk.ac.uk*
[b] *Department of Chemistry, University of Exeter, Exeter, UK EX4 4QD*
[c] *Department of Chemistry, University College London, Christopher Ingold Laboratories, 20 Gordon Street, London, UK WC1H 0AJ*

Received 12th January 2000, Accepted 8th March 2000
Published on the Web 30th March 2000

The trimethylplatinum(IV) complexes of a number of dithiocarbamato ligands have been prepared. The complexes are dimeric in the solid state and in solution, with the ligands acting in both a bridging and chelating fashion. Restricted rotation about the ligand C–N bonds in solution leads to the formation of four rotomers. The kinetics of the restricted rotation was measured by a variety of dynamic NMR techniques in the slow and intermediate exchange regimes. Two distinct processes are observed, namely the independent rotation about each C–N bond and correlated rotation about both C–N bonds. The free energies of activation, which are strongly dependent on the nature of the ligand substituents, are in the range 65–88 kJ mol^{-1} at 298 K. The origins of the barrier to rotation and the effects of the nitrogen substituents are discussed. The crystal structures of *fac*-$[PtMe_3(Me_2NCS_2)]_2$ and *fac*-$[PtMe_3(Ph(H)NCS_2)]_2$ are reported.

Introduction

Restricted rotation about the amide C–N bond is of interest because it plays an important role in helping to determine the secondary and tertiary structures of peptides,[1] and the origins of the barrier have been the subject of a number of recent theoretical studies.[2–6]

Classically, resonance structures (Scheme 1) have been used

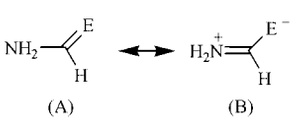

Scheme 1

to rationalise the barrier to C–N bond rotation in amides and related systems:[7] the greater the contribution of structure (**B**), the higher is the barrier to rotation. Factors that lead to the stabilisation of (**B**), such as electron donating substituents on nitrogen or electron withdrawing carbon substituents, should lead to an increase in the barrier to rotation. One of the main objections to the resonance model is its apparent failure to predict the relative barrier heights to rotation in formamide and thioformamide. As oxygen is more electronegative than sulfur, structure (**B**) should be more stable in $H_2NC(O)H$ than $H_2NC(S)H$. Formamide might therefore be expected to exhibit the higher barrier to C–N bond rotation, but the experimentally measured barrier is lower.[8–11] The observed trend in the activation energies can in fact be rationalised on the basis of the resonance model if π basicity is also considered. Oxygen is more π-basic than sulfur and consequently structure (**A**) (Scheme 1) will be more stable in $H_2NC(O)H$ than $H_2NC(S)H$. The barrier to rotation thus depends on the balance between the electronegativity and the π basicity. Studies on monothiocarbamates indicate π basicity is dominant,[12] suggesting that the barrier should actually be higher in thioformamide than formamide.

Recent theoretical studies on the origins of the rotational barrier in amides, based on Atoms in Molecules theory,[13] have cast doubt on the validity of the resonance model. According to the Atoms in Molecules theory the barrier to a conformational rearrangement depends on the net change in the attractive (V_a) and repulsive (V_r) forces within molecules.[14] The barrier to C–N bond rotation in amides is thus thought to arise as a result of a large decrease in the attractive forces at the nitrogen atom as it becomes pyramidal in the transition state. There is a small reduction in repulsive forces in the transition state, but this is insufficient to offset the decrease in V_a. Substituents on the carbonyl carbon atom that are able to donate electron density to the sp^2 hybridised nitrogen, through the σ framework, in the planar ground state, are therefore expected to increase the rotational barrier; the decrease in V_a will be greater on going to the transition state. This model readily explains the relative barrier heights to C–N bond rotation in formamide and thioformamide. The C(S)H group is more polarisable than the C(O)H group and can therefore donate more electron density to nitrogen in the ground state. Furthermore, calculations indicate little change in the C=O or C=S bond lengths on rotation, inconsistent with a resonance model.

The conclusions of the Atoms in Molecules analysis have been challenged on theoretical grounds[15] and recent experimental work aimed at testing the model was inconclusive.[16]

Dithiocarbamates are important and versatile compounds that find widespread use as fungicides, bactericides, for the vulcanisation of rubber and in the petrochemical industry.[17] Metal complexes of dithiocarbamates are used to prepare metal sulfide thin films by metal–organic chemical vapour deposition (MOCVD)[18] and in regenerative solar cell technology to improve light-to-electrical energy conversion.[19] Like amides, dithiocarbamates exhibit restricted C–N bond rotation[20] and provide another experimental model for probing the origins of the rotational barrier. We report here the results of an experimental dynamic NMR study on C–N bond rotation in trimethylplatinum(IV) complexes of dithiocarbamates. These

DOI: 10.1039/b000264j

complexes were chosen because they are stable and provide suitable NMR handles on the stereodynamics.

Experimental

Materials

Starting materials were purchased from Aldrich Chemical Company and used without further purification. Trimethylplatinum(IV) sulfate was prepared by our published method.[21] The dithiocarbamate ligands were all prepared similarly, as illustrated by the procedure for ethylammonium *N*-ethyldithiocarbamate.

Ethylammonium *N*-ethyldithiocarbamate. The reaction was carried out under an atmosphere of dry, oxygen-free nitrogen using standard Schlenk techniques. 20 cm^3 of a 2.0 mol dm^{-3} methanolic solution of ethylamine were added dropwise to a diethyl ether solution of carbon disulfide (1.5 cm^3 in *ca.* 5 cm^3 of Et_2O). The resulting solution was stirred for *ca.* 1 h. The product was precipitated by the addition of 100 cm^3 of diethyl ether and isolated by filtration. No further purification was necessary. Yield 2.86 g (86%).

Complexes. All procedures were performed in the dark, to prevent the photoreduction of the trimethylplatinum(IV) group. In a typical experiment, an aqueous solution of the appropriate ligand (in small excess) was added to a stirred aqueous solution of trimethylplatinum(IV) sulfate. A dense white precipitate of the complex formed immediately. The product was isolated by filtration, dried in air, and crystallised at ambient temperature from a benzene–light petroleum (bp 60–80 °C) mixture. Analytical data are reported in Table 1.

Physical methods

Hydrogen-1 NMR spectra were recorded on either a Bruker AMX400 or AMX600 Fourier transform spectrometer, operating at 400.13 and 600.13 MHz, respectively; chemical shifts are quoted relative to tetramethylsilane as an internal standard. Solution ^{195}Pt NMR spectra were recorded on the same instruments, operating at 85.75 and 128.63 MHz, respectively; chemical shifts are quoted relative to the absolute frequency scale, $\Xi(^{195}Pt) = 21.4$ MHz. Probe temperatures, controlled by standard B-VT 2000 units, were checked periodically against a standard sample of ethylene glycol, and are considered accurate to ±1 K. Probe temperatures were allowed to equilibrate for *ca.* 15 min before the acquisition of each spectrum. Band shapes were analysed (non-iteratively) using the program DNMR 5.[22] The solid-state CPMAS ^{195}Pt NMR spectrum of complex **7** was obtained by Dr A. E. Aliev on a Bruker MSL300 Fourier transform spectrometer, operating at 64.4 MHz.

Hydrogen-1 two-dimensional exchange (EXSY) spectra were obtained using the Bruker automation program NOESYTP, which generates the pulse sequence D1–90°–D0–90°–D8–90°–free induction decay. Spectra were recorded typically with 2048 and 512 words of data in f_2 and f_1, respectively. The initial delay, D0, was 3 μs and relaxation delay, D1, was 5.0 s. The mixing time, D8, was varied according to the complex under investigation and the experimental temperature. Exchange rates were extracted from the resulting two-dimensional intensity matrix using the program D2DNMR.[23] The ^{195}Pt EXSY NMR spectrum of complex **7** was acquired at 333 K on the Bruker AMX400 instrument (see above) using the NOESYTP program, which was modified to enable ^{1}H decoupling in f_1 and f_2. The relaxation delay, D1, was 2 s, the initial variable delay, D0, was 3 μs, and the mixing time, D8, was 0.1 s. The spectrum was acquired with 256 words of data in f_1 and 4096 words of data in f_2, and a spectral width of *ca.* 350 ppm in both domains.

Hydrogen-1 and ^{195}Pt spin–lattice relaxation data were obtained using the inversion-recovery technique[24] (Bruker automation programs T1IR and T1IRPG) and analysed using the program T1CALS.[25] Selective inversion experiments were carried out using our program SOFTPULV, which generates the pulse sequence D1–180°–U-BURP256–VD–90°– free induction decay. The soft U-BURP256 pulse[26] was centred on the peak to be inverted. The relaxation delay, D1, was 10 s for the ^{1}H experiments and 2 s for the ^{195}Pt experiments. The VD list contained typically 16–20 delays. Exchange rates were extracted from the longitudinal magnetisations using the program CIFIT.[27] Rate constants obtained from the dynamic NMR spectra were used to calculate the Eyring activation parameters; errors quoted are those defined by Binsch and Kessler.[28]

Infrared spectra were recorded as pressed KBr discs on a Nicolet Magna 205 FT-IR spectrometer, operating in the range 4000–400 cm^{-1}. Mass spectra (LSIMS) were obtained at the London School of Pharmacy, on a VG Analytical ZAB-SE4F Instrument. Elemental analyses were performed at University College.

Crystallography

Single crystals of the complexes $[PtMe_3(Me_2NCS_2)]_2$ **2** and $[PtMe_3(Ph(H)NCS_2)]_2$ **6** were obtained as described above and mounted on glass fibres. Geometric and intensity data were obtained using an automatic four-circle Nicolet R3mV diffractometer, using the ω–2θ technique at 293(2) K. Three standard reflections, remeasured every 97 scans, showed no significant loss of intensity during the data collection of either sample. Data were corrected using routine procedures and empirical absorption corrections applied (Ψ scan method). The structures were solved by direct methods and refined to convergence by least squares (SHELXL 93).[29] Crystal data, collection parameters, and refinement parameters are reported in Table 2.

CCDC reference number 186/1892.

See http://www.rsc.org/suppdata/dt/b0/b000264j/ for crystallographic files in .cif format.

Results

Complexes **1**–**7** were prepared as described above and isolated as air-stable, crystalline solids. Infrared spectra show three bands in the region 3000–2800 cm^{-1}, characteristic of a *fac* octahedral $[PtMe_3]^+$ moiety.[21] The C–S and C–N stretching modes of the dithiocarbamato ligands are also readily identified;[30] the positions of the C–N stretching bands indicate an intermediate bond order between one and two.[30] Bands show little dependence on the nature of the ligand. Liquid secondary ion mass spectrometry (LSIMS) was performed on all complexes and, with the exception of **2** and **4**, which completely fragmented on ionisation, good spectra were obtained. The highest observed mass/charge peaks correspond to species of general formula $[PtMe_3(dtc)]_2$ (dtc = dithiocarbamate), indicat-

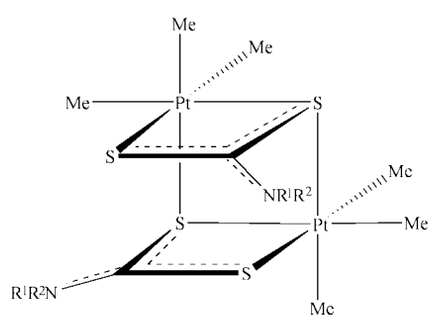

Complex	1	2	3	4	5	6	7
R^1	H	Me	Et	Me	Et	Ph	Ph
R^2	H	Me	Et	H	H	H	Me

Table 1 Analytical data for complexes **1**–**7**

Complex	Yield[a]	Mass spectral data[b]	Infrared data[c]/cm^{-1}					Analysis[d] (%)		
			ν(N–H)	ν(C–H)	ν(C–N)	ν(C–S)	ν(Pt–C)	C	H	N
1	75	665 $[M + H]^+$ 649 $[M - CH_3]^+$ 619 $[M - 3CH_3]^+$	3344 3259 3177 1609	2965 2899 2805	1609	848 615	596	15.19(14.45)	3.36(3.34)	4.07(4.22)
2	61			2947 2896 2800	1530	968		20.29(19.99)	4.13(4.20)	3.86(3.89)
3	54	776 $[M]^+$ 761 $[M - CH_3]^+$ 731 $[M - 3CH_3]^+$		2964 2895 2806 2800	1516	990	555	24.78(24.73)	4.96(4.94)	3.53(3.61)
4	85		3267	2960 2891 2803	1517	968 619	556	17.42(17.34)	3.71(3.79)	3.96(4.04)
5	57	705 $[M - CH_3]^+$ 675 $[M - 3CH_3]^+$ 630 $[M - 6CH_3]^+$	3266	2961 2892 2804	1518	969 615	534	20.13(19.99)	4.17(4.20)	3.81(3.89)
6	60	816 $[M]^+$ 801 $[M - CH_3]^+$ 771 $[M - 3CH_3]^+$	3248	2954 2897 2853	1527	976	588	30.04(29.40)	3.74(3.71)	3.29(3.43)
7	71	844 $[M]^+$ 829 $[M - CH_3]^+$ 799 $[M - 3CH_3]^+$		2956 2895 2806	1489	974 620	549	31.30(31.27)	4.03(4.06)	3.24(3.32)

[a] Percentage yield relative to $[Pt(CH_3)_3]_2SO_4 \cdot 4H_2O$. [b] LSIMS technique. [c] Recorded as pressed KBr discs; not all bands observed. [d] Calculated figures in parentheses.

Table 2 X-Ray data[a] for complexes **2** and **6**

	2	**6**
Formula	$C_{12}H_{30}N_2Pt_2S_4$	$C_{20}H_{30}N_2Pt_2S_4$
M_r	720.80	816.68
Point group	Orthorhombic	Monoclinic
Space group	*Pccn*	$P2_1/c$
Radiation	Mo-Kα (λ = 0.71073 Å)	Mo-Kα (λ = 0.71073 Å)
a; b; c/Å	10.106(2); 10.656(2); 19.655(4)	10.611(2); 17.725(4); 14.373(3)
α; β; γ/°		90.0; 94.37(3)
U/Å^3	2116.6(7)	2695.4(10)
D_c/mg m^{-3}	2.262	2.013
μ/mm^{-1}	13.592	10.687
Data collection range/°	$2.78 < \theta < 25.06$	$2.57 < \theta < 25.06$
Reflections collected	3550	4750
Unique (R_{int})	1866 (0.100)	4485 (0.0295)
R [$I > 2\sigma(I)$]	0.0522	0.0590
$wR2$ [$I > 2\sigma(I)$]	0.1322	0.1316
R (all data)	0.0774	0.1179
$wR2$ (all data)	0.1846	0.2103

[a] Estimated standard deviation in parentheses.

ing the presence of dimeric species. The observed isotope distribution patterns are in accordance with those calculated for the proposed species. Analytical data are reported in Table 1.

Crystal structures of complexes 2 and 6

Dithiocarbamates are able to stabilise metal centres in a number of ways.[31] The trimethylplatinum(IV) cation usually forms dimeric complexes of the type *fac*-$[PtMe_3L]_2$ [32–36] with anionic donors, such as acetylacetonates. Mass spectral data indicate that the trimethylplatinum(IV) dithiocarbamato complexes, **1**–**7**, also form dimeric species (see above). The crystal structures of **2** and **6** (Fig. 1) were obtained to confirm the presence of dimers in the solid state. The structures show clearly that the ligands act in both a chelating and bridging fashion, giving C_2-symmetric dimers; the nature of the ligand substituents does not affect the molecular structure. In both complexes the ligand C–N distances are intermediate between single and double bonds and the nitrogen atoms are planar (sum of the bond angles is ≈360°). Selected bond distances and angles are reported in Table 3.

NMR studies

Hydrogen-1 and ^{195}Pt NMR spectroscopic data indicate that the trimethylplatinum(IV) dithiocarbamato complexes, **1**–**7**, are also dimeric in solution. The dimers presumably retain the C_2-symmetric configuration observed in the solid state. There is no evidence of monomeric or any other dimeric species in solution.

Complexes 1–3. The *static* ^{1}H NMR spectra of the complexes of the symmetrically substituted dithiocarbamato ligands, **1**–**3**, display signals due to the dithiocarbamato substituents and the platinum–methyl groups. The two dithiocarbamato ligands are related by a C_2-axis and are indistinguishable in the NMR experiment, but because there is no plane of symmetry along the C–N bonds the two substituents on nitrogen are inequivalent. The NMR spectra of the complexes thus display two

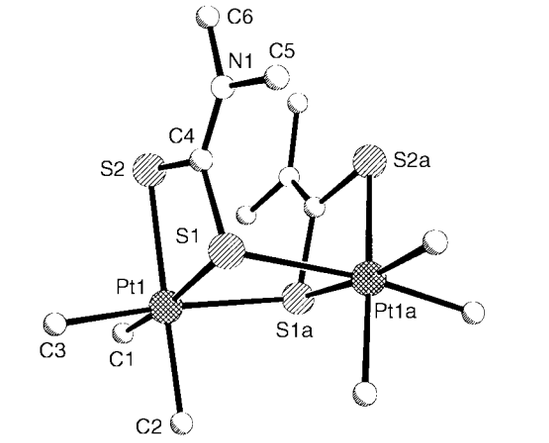

(2)

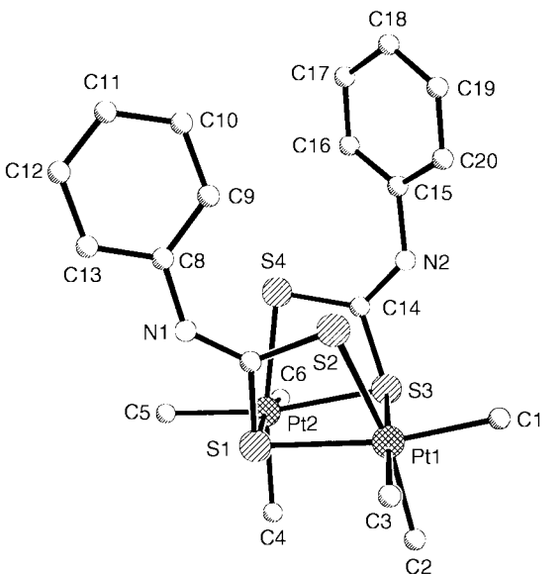

(6)

Fig. 1 Molecular structures of complexes **2** and **6**, showing the atom labelling schemes.

Table 3 Selected bond lengths (Å) and angles (°) for complexes **2** and **6**[a]

2		**6**	
Pt(1)–S(1)	2.574(4)	Pt(1)–S(1)	2.517(5)
Pt(1)–S(2)	2.490(4)	Pt(1)–S(2)	2.489(5)
Pt(1)–C(1)	2.10(2)	Pt(1)–C(1)	2.09(2)
Pt(1)–C(2)	2.09(2)	Pt(1)–C(2)	2.08(2)
Pt(1)–C(3)	2.09(2)	Pt(1)–C(3)	2.05(3)
S(1)–C(4)	1.77(2)	S(1)–C(7)	1.79(2)
S(2)–C(4)	1.71(2)	S(2)–C(7)	1.71(2)
N(1)–C(4)	1.34(2)	N(1)–C(7)	1.33(3)
N(1)–C(5)	1.49(3)	N(2)–C(14)	1.35(3)
N(1)–C(6)	1.47(2)	N(1)–C(8)	1.43(2)
S(1)–Pt(1)–S(2)	71.78(14)	S(1)–Pt(1)–S(2)	71.9(2)
S(1)–C(4)–S(2)	115.1(10)	S(3)–Pt(2)–S(4)	72.0(2)
C(1)–Pt(1)–S(1)	172.3(5)	S(1)–C(7)–S(2)	114.5(11)
C(2)–Pt(1)–S(2)	173.0(6)	C(1)–Pt(1)–S(1)	170.1(8)
C(4)–N(1)–C(6)	122(2)	C(2)–Pt(1)–S(2)	169.9(8)
C(5)–N(1)–C(6)	118.1(14)	C(7)–N(1)–C(8)	132(2)

[a] See Fig. 1 for atom labelling scheme; estimated standard deviations given in parentheses.

equally intense sets of signals in the dithiocarbamato region and three equally intense signals, with ^{195}Pt satellites ($^{2}J_{PtH} \approx 70$ Hz), in the platinum–methyl region. The ^{1}H NMR spectrum of $[PtMe_3(Me_2NCS_2)]_2$ **2** is shown in Fig. 2 and ^{1}H NMR data are

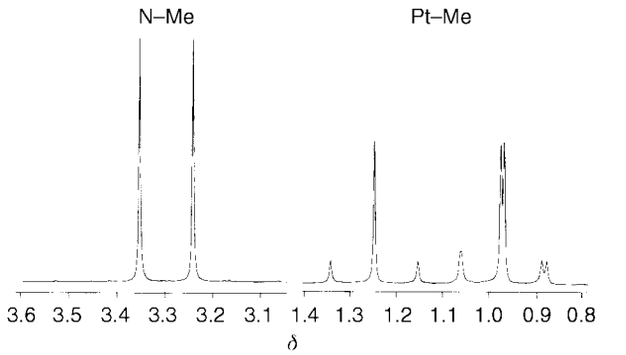

Fig. 2 400 MHz ^{1}H NMR spectrum of $[PtMe_3(Me_2NCS_2)]_2$ **2** at 298 K.

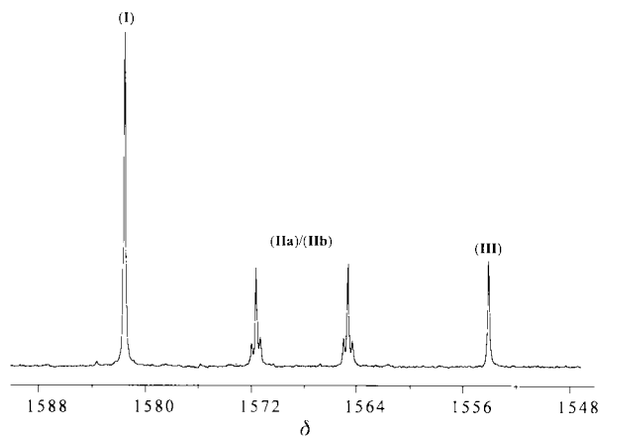

Fig. 3 128 MHz ^{195}Pt NMR spectrum of complex **7** in $CDCl_3$ at 298 K.

reported in Table 4. The *static* ^{195}Pt NMR spectra of complexes **1**–**3** each display a single resonance (Table 5).

Restricted rotation about the C–N bonds of the dithiocarbamato ligands leads to the formation of four degenerate rotomers in solution; these are depicted in Scheme 2. Rotation about the C–N bonds exchanges the dithiocarbamato N substituents and can readily be monitored by ^{1}H dynamic NMR spectroscopy. The complexes display signs of irreversible decomposition at elevated temperatures, frustrating accurate analysis of the ^{1}H DNMR line shapes. The exchange kinetics was therefore measured in the slow exchange regime by either two-dimensional exchange spectroscopy (EXSY)[23,37] or selective inversion experiments,[38–41] as appropriate. Eyring activation parameters are reported in Table 6.

Complexes 4–7. Restricted rotation about the C–N bonds in the complexes of the unsymmetrically substituted dithiocarbamato ligands, **4**–**7**, also leads to the formation of four rotomers (Scheme 2), three of which are chemically distinct. This is seen clearly in the ^{195}Pt NMR spectra of the complexes. The two platinum atoms are equivalent in rotomers (**I**) and (**III**) (Scheme 2) and each therefore gives a single signal. Rotomers (**I**) and (**III**) are distinguished readily on the basis of their relative intensities; (**I**) is the more abundant species (see below). In the degenerate pair of rotomers, (**IIa**)/(**IIb**), the C_2-symmetry of the molecule is broken and the two platinum atoms are chemically distinct, giving two equally intense lines, with ^{195}Pt satellites. The observation of ^{195}Pt satellites is conclusive evidence that the complexes exist as dimers in solution. The ^{195}Pt NMR spectrum of $[PtMe_3(Ph(Me)NCS_2)]_2$ **7** is shown in Fig. 3 and ^{195}Pt NMR data are reported in Table 5.

The ^{1}H NMR spectra of complexes **4**–**7** display three sets of resonances of differing intensities, due to rotomers (**I**), (**IIa**)/(**IIb**), and (**III**). The spectra of all four complexes are analogous and the example of complex **7**, $[PtMe_3(Ph(Me)NCS_2)]_2$, will

Table 4 Hydrogen-1 NMR data[a] for complexes **1**–**7**

Complex	Rotamer	Population(%)	δ Pt–CH_3[b]	δ ligand	
				R^1	R^2
1[c]			0.71(73); 0.80(71); 1.13(76)	8.62	9.05
2			0.94(≈70); 0.94(≈70); 1.22(76)	3.22	3.34
3			0.89(73); 0.91(71); 1.20(75)	1.27;[d] 3.47;[d,e] 3.90;[d,e]	1.36;[d] 3.56;[d,e] 3.92[d,e]
4[f]	**(I)**	67	0.87(74); 0.90(71); 1.18(75)	3.19[g]	7.00[g]
	(IIa)/**(IIb)**	15/15	0.86(74); 0.93(73); 0.99(72); 1.19 (76); 1.27(76)	3.03[g] 3.19[g]	7.37[g] 6.99[g]
	(III)	3		3.01[g]	7.40[g]
5[f]	**(I)**	70	0.87(73); 0.92(75); 1.22(75)	1.28;[d] 3.57;[d-f] 3.72[d,e,g]	6.82[g]
	(IIa)/**(IIb)**	13/13	0.85; 0.90; 0.91; 0.98; 1.21	1.27;[d] 3.42;[d,e,g] 3.64[d,e,g]	6.82[g]
				1.18;[d] 3.60;[d,e,g] 3.72[d,e,g]	7.21[g]
	(III)	4		—	7.26[g]
6[f]	**(I)**	76	0.99(≈70); 0.99(≈70); 1.30(72)	7.2–7.7	8.48
	(IIa)/**(IIb)**	11/11	0.03(74); 0.84(71); 0.95(72); 0.98; 1.18(75); 1.35(75)	7.2–7.7 7.2–7.7	8.48 8.85
	(III)	3	0.02; 0.79(71); 1.21	7.2–7.7	8.88
7	**(I)**	46	0.98(69); 1.01(64); 1.30(76)	7.1–7.6	3.45
	(IIa)/**(IIb)**	20/20	−0.02(73); 0.70(70); 0.97(69); 1.06(73); 1.09(76); 1.35(76)	7.1–7.6 7.1–7.6	3.56 3.59
	(III)	14	0.07(74); 0.66(71); 1.14(76)	7.1–7.6	3.77

[a] Spectra recorded at 298 K in $(CDCl_2)_2$, except [c-f]; chemical shifts quoted relative to tetramethylsilane; not all signals resolved. [b] $^2J_{PtH}$/Hz given in parentheses. [c] Recorded in $(CD_3)_2CO$ at 298 K. [d] $^3J_{HCCH} \approx 7$ Hz. [e] $^2J_{HCH} \approx 14$ Hz. [f] Recorded at 263 K. [g] $^3J_{HCNH} \approx 5$ Hz.

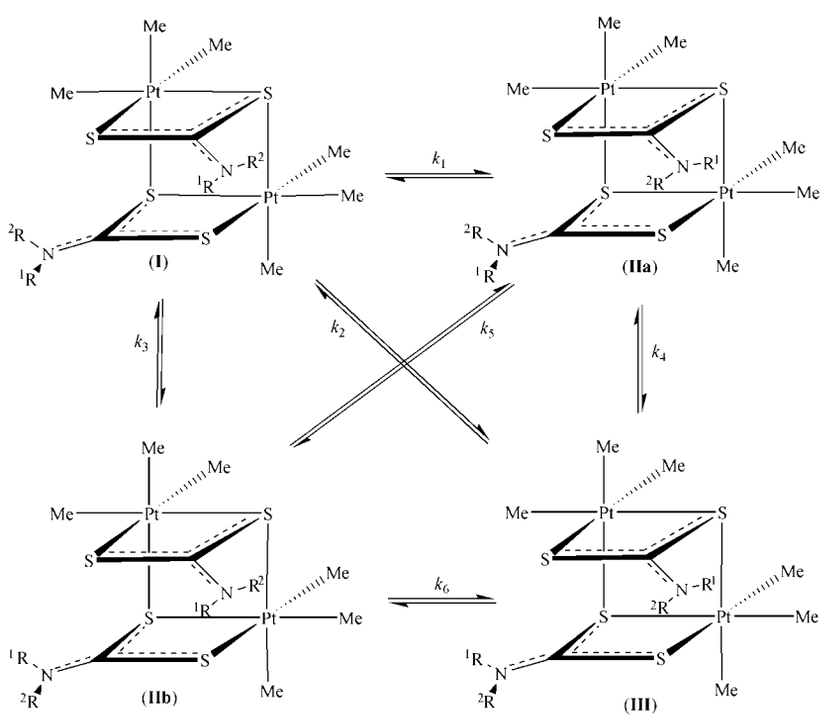

Scheme 2 The four rotomers of complexes **1**–**7** and the possible interconversion pathways between them. Note $k_1 = k_3$ and $k_4 = k_6$.

serve to illustrate the analysis of the problem. The ambient temperature ^{1}H NMR spectrum of **7** displays signals in three regions, namely the platinum–methyl region (*ca.* δ −0.5 to 1.5), the ligand-methyl region (*ca.* δ 3.4–3.8), and the aromatic region (*ca.* δ 7.1–7.6).

The platinum–methyl region displays twelve signals, with ^{195}Pt satellites ($^2J_{PtH} \approx 70$ Hz). Rotomers **(I)** and **(III)** each give three equally intense Pt–Me signals, and are easily distinguished on the basis of their relative chemical shifts; one of the equatorial Pt–Me groups of rotomer **(III)** lies within the shielding current of the dithiocarbamato phenyl ring and is consequently shifted to lower frequency. All six Pt–Me groups are inequivalent in **(IIa)**/**(IIb)**, giving six equally intense resonances, one of which is shifted to lower frequency by the shielding current of one of the phenyl rings. The ligand-methyl region displays four signals: rotomers **(I)** and **(II)** each give a single signal, while **(IIa)**/**(IIb)** give a pair of equally intense signals. The relative abundance of the rotomers (Table 4), determined by integration of the N–Me resonances, is in the order **(I)** > **(IIa)** = **(IIb)** > **(III)**. The aromatic region of the spectrum is highly complex owing to the overlap of the N-phenyl resonances of the different rotomers, frustrating a full assignment. It is difficult to distinguish unambiguously between rotomers **(I)** and **(III)** and **(IIa)** and **(IIb)** in complexes **4** and **5** (*i.e.* when no phenyl group is present); the assignments given in Tables 4 and 5 may be reversed. This does not affect the analysis of the

stereodynamics. Hydrogen-1 NMR data for complexes **4**–**7** are reported in Table 4.

On warming, reversible band shape changes were observed in all regions of the spectrum, indicating the onset of C–N bond rotation at a measurable rate. The N–Me signals provide the most suitable spectroscopic handle, so were used for the measurement of the exchange kinetics. The complex displays signs of irreversible decomposition at higher temperatures, so rates were obtained from magnetisation transfer experiments (EXSY). The EXSY spectrum of **7** (Fig. 4) displays cross-peaks due to exchange between pairs of rotomers, namely **(I)** $\rightleftharpoons$ **(IIa)**/**(IIb)** and **(IIa)**/**(IIb)** $\rightleftharpoons$ **(III)** as a consequence of rotation around the C–N bond of *one* of the dithiocarbamato ligands. Cross-peaks are also observed between rotomers **(I)** and **(III)**, due to magnetisation transfers that result either from the correlated rotation of both dithiocarbamato C–N bonds or the stepwise rotation about first one C–N bond, then the other. For an equilibrium process of the type shown in Scheme 3, the stepwise rate constant, k_{AC}, is given by eqn. (1)

$$\mathrm{A} \underset{k_{-1}}{\overset{k_1}{\rightleftharpoons}} \mathrm{B} \underset{k_{-2}}{\overset{k_2}{\rightleftharpoons}} \mathrm{C}$$

Scheme 3

$$k_{AC} = \frac{k_1 k_2}{k_{-1} + k_{-2}} \qquad (1)$$

where $k_1 = k$[**(I)** ⟶ **(II)**] and $k_2 = k$[**(II)** ⟶ **(III)**]. The experimentally measured rates, k[**(I)** ⟶ **(III)**], are greater than the rates calculated for a stepwise process at all temperatures measured. Thus, although a significant contribution from the stepwise exchange to the observed magnetisation transfers is likely, data clearly show that correlated rotation about both dithiocarbamato C–N bonds is occurring, interchanging rotomer **(I)** and **(III)**.

Table 5 Platinum-195 NMR data[a] for complexes **1**–**7**

Complex	T/K	δ **(I)**	δ **(IIa)**/**(IIb)**[b]	δ **(III)**
1[c]	298	1416		
2	298	1577		
3	298	1564		
4	233	1623	1609, 1598 (80)	1587
5	233	1626	1609, 1607 (80)	1596
6	233	1632	1600, 1587 (76)	1582
7	298	1584 1601[d]	1575, 1569 (87)	1559

[a] Chemical shifts quoted relative to the absolute frequency scale $\Xi(^{195}\mathrm{Pt}) = 21.4$ MHz; data recorded in $CDCl_3$ except [c]; see Scheme 2 for rotomer labelling. [b] $^2J_{PtPt}$/Hz given in parentheses. [c] Recorded in $(CD_3)_2CO$. [d] Solid-state CPMAS NMR data, δ_{11} 989, δ_{22} 1502, δ_{33} 2306, $\Delta\sigma = -1060$ ppm, $\eta = 0.73$ (CSA tensors assigned according to Haeberlen's convention).[48]

Correlated rotation about both C–N bonds in **(II)**, exchanging rotomers **(IIa)** and **(IIb)**, is also possible. In principle this can also be followed by ^{1}H EXSY experiments, but the signals due to **(IIa)**/**(IIb)** are not sufficiently well separated to enable EXSY cross-peaks between them to be characterised properly. Kinetic data were therefore sought by ^{195}Pt exchange NMR spectroscopy. The acquisition of an informative two-dimensional ^{195}Pt EXSY spectrum was not immediately successful. Several experiments had to be performed (at higher temperatures) with reduced mixing times before a suitable spectrum was obtained. The ^{195}Pt EXSY spectrum of complex **7** shows cross-peaks between the signals due to **(IIa)**/**(IIb)**. Quantitative data were not obtained, but from the relative cross-peak intensities it is clear that the rate of magnetisation transfer, k[**(IIa)** $\rightleftharpoons$ **(IIb)**], is of the same order of magnitude as for the **(I)** $\rightleftharpoons$ **(III)** process, indicating that correlated rotation about both C–N bonds is occurring.

The problems of acquiring an informative ^{195}Pt EXSY spectrum were thought to arise because of rapid spin–lattice relaxation. Rates of relaxation were therefore measured using the standard inversion-recovery technique[24] and found to be very rapid. Platinum-195 relaxation is usually dominated by either the spin-rotation (SR) mechanism or chemical shift anisotropy (CSA) mechanism[42,43] and relaxation rates were measured under various conditions to try to distinguish them. Data,

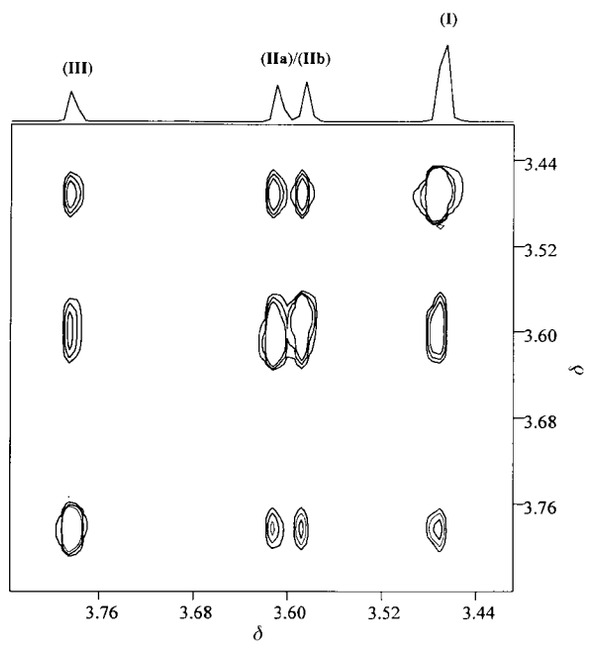

Fig. 4 400 MHz ^{1}H two-dimensional exchange (EXSY) spectrum of $[PtMe_3(Ph(Me)NCS_2)]_2$ **7** at 323 K, showing the N–Me region. Cross-peaks are observed between rotomers **(I)** and **(IIa)**/**(IIb)**, **(IIa)**/**(IIb)** and **(III)**, and **(I)** and **(III)**.

Table 6 Activation parameters[a] for complexes **1**–**7**

Complex	Process[b]	$\Delta H^{\ddagger}$/kJ mol^{-1}	$\Delta S^{\ddagger}$/J K^{-1} mol^{-1}	$\Delta G^{\ddagger}$/kJ mol^{-1}
1[c]		75.01(3.35)	12.02(10.76)	71.43(0.14)
2		83.63(1.98)	7.0(6.0)	81.54(0.19)
3		123.81(9.89)	[d]	82.89(0.56)
4	[e]	82.01(0.77)	12.02(2.41)	72.27(0.05)
5	[e]	55.51(0.80)	−36.40(2.63)	66.36(0.01)
6	[e]	73.29(1.03)	25.78(3.39)	65.61(0.01)
7[f]	**(I)** ⟶ **(IIa)**/**(IIb)**	86.81(2.37)	1.22(6.98)	86.45(0.29)
	(IIa)/**(IIb)** ⟶ **(III)**	82.51(2.21)	−15.88(6.51)	87.24(0.27)
	(I) ⟶ **(III)**	83.73(2.81)	−11.49(8.27)	87.15(0.35)

[a] Errors given in parentheses; $\Delta G^{\ddagger}$ quoted at 298 K. Data measured on $(CDCl_2)_2$ solutions of the complexes except [c]. [b] See Scheme 2 for labelling. [c] Data measured in $(CD_3)_2CO$. [d] Data not reported (unreliable due to narrow temperature range). [e] Spectra were simulated using equal rate constants for the four independent rate processes (see Scheme 2). [f] No quantitative data obtained for the process **(IIa)** ⟶ **(IIb)** (see text).

Table 7 Spin–lattice relaxation times[a] for complex **7**

Field/T	*T*/K	Solvent	Rotomer (I)	(IIa)/(IIb)	(IIa)/(IIb)	(III)
6.3	303	$(CDCl_2)_2$	215	241	211	251
		$CDCl_3$	552	607	554	639
	323	$(CDCl_2)_2$	346	377	339	400
		$CDCl_3$	683	740	686	744
9.4	303	$(CDCl_2)_2$	110	110	98	126
		$CDCl_3$	266	297	259	309
	323	$(CDCl_2)_2$	154	170	145	180
		$CDCl_3$	326	376	343	405
11.8	303	$(CDCl_2)_2$	66	77	64	79
		$CDCl_3$	179	210	176	215
	323	$(CDCl_2)_2$	98	111	95	117
		$CDCl_3$	230	257	227	269
14.1	303	$(CDCl_2)_2$	43	47	42	51
		$CDCl_3$	120	129	117	143
	323	$(CDCl_2)_2$	65	70	63	76
		$CDCl_3$	159	172	153	183

[a] Spin–lattice relaxation times ($\times 10^{-3}$ s); errors *ca.* ±5%; see Scheme 2 for rotomer labelling.

collected in Table 7, are consistent with the CSA mechanism being dominant. This is supported by the solid-state ^{195}Pt CPMAS NMR spectrum of complex **7**, which indicates a large chemical shielding anisotropy: $\Delta\sigma = -1060$ ppm (Table 5). Small contributions from other mechanisms are also apparent.[42,43]

Reliable rate data for the C–N bond rotations were measured for complexes **4**–**7** by band shape analysis or magnetisation transfer experiments. Data were used to calculate the Eyring activation parameters, which are reported in Table 6.

Discussion

The trimethylplatinum(IV) dithiocarbamato complexes, **1**–**7**, exist as dimers in the solid state and in solution. In solution, restricted rotation about the dithiocarbamato C–N bonds leads to the formation of four rotomers. The kinetics of C–N bond rotation was measured by DNMR spectroscopy and activation data are reported in Table 6. The free energies of activation, the most reliable measure of the energetics, show a dependence on the nitrogen substituents of the dithiocarbamato ligand, particularly when an alkyl or aryl group is substituted by hydrogen; substitution leads to a significant decrease in $\Delta G^{\ddagger}$ (at 298 K). Complex **1**, $[PtMe_3(H_2NCS_2)]_2$, might therefore be predicted to have the lowest barrier to C–N bond rotation. The higher than expected barrier in **1** (Table 6) probably results because of the more polar solvent system [complex **1** was studied in acetone because of its poor solubility]. Polar solvents, such as acetone and DMSO, have been shown to increase barriers to C–N bond rotation.[44–46] The solvent effect arises because there is a large decrease in the dipole moment on rotation and consequently polar solvents destabilise the transition state.[44–46]

Classically, a resonance model has been used to rationalise the barrier to C–N bond rotation in amides and related systems, such as dithiocarbamates.[7] The barrier is presumed to arise because of a contribution from (**B**) (Scheme 1) to the overall structure. The amount of nitrogen π donation will be affected by the substituents on N; electron-donating substituents should increase π donation and hence the barrier to rotation. Thus the rotational barrier would be expected to increase when H is substituted for an alkyl group. This is the case (Table 6). Correlated rotation around both C–N bonds (see above) provides some evidence of delocalisation. For the correlated process to occur there must be communication between the two dithiocarbamato ligands in the dimer. This is thought most likely to occur either *via* the platinum centres or as a result of through space interactions between the non-bridging S atom of one of the dithiocarbamato ligands and the C(S) atom of the other [the S···C distance ≈ 3.28 Å (*cf.* sum of van der Waals radii = 3.55 Å)].

The resonance model has been called into question. Recent calculations using Atoms in Molecules theory indicate that the barrier to C–N bond rotation results from the loss of attractive potential, V_a, at N as a consequence of the C–N bond lengthening on rotation.[2–6] Electron donating substituents on nitrogen will increase the attractive potential at nitrogen in the ground state and are therefore expected to increase the barrier to rotation. The loss of attractive potential is offset slightly by a small reduction in the repulsive interactions between the nitrogen substituents in the (pyramidal) transition state. The net effect of the nitrogen substituents on the rotational barriers will depend on the balance between their electronic and steric effects. The effect of hydrogen substitution on the barrier can readily be rationalised using this model. With small substituents, such as hydrogen, the reduction in repulsive forces on pyramidalisation will, presumably, be minimal and the barrier height will depend (essentially) on the change in attractive potential only. Since hydrogen is a poorer σ donor than alkyl (or aryl) groups, the attractive potential at N in the ground state will decrease on substitution with H and the barrier to rotation will be lowered. A more detailed rationalisation of the observed trend in the free energies is problematic because the net effects of the different nitrogen substituents are not precisely known.

The effect of metal co-ordination on the C–N rotation kinetics cannot be determined. Assuming that there are no unfavourable steric interactions between the nitrogen substituents and the metal moiety (which appears to be the case from the crystal structures), any co-ordination effect will presumably be constant for all complexes. Preliminary studies by our group on (free) selenothiocarbamate ligands and their trimethylplatinum(IV) complexes, $[PtMe_3(R^1R^2NC(S)Se)]_2$, suggest that co-ordination has only a minimal effect on the energetics. This is in contrast to recent work on the tricarbonylrhenium(I) complexes of pyridine-2,6-bis(*N*,*N*-dialkylcarbothioyl amide, $C_5H_3N(C(S)NR_2)_2$-2,6) (L), $[ReX(CO)_3(L)]$ (X = Cl, Br, or I), which show that co-ordination of carbothioyl group to the metal centre reduces the barrier to C–N bond rotation significantly.[47]

Conclusion

The results obtained on the restricted C–N bond rotations in the dithiocarbamato complexes, **1**–**7**, do not provide any conclusive experimental evidence in support of either model (see above), but some evidence of delocalisation is provided by the correlated rotation about the C–N bonds of both dithiocarbamato ligands. A detailed theoretical study on origin of the barrier and the effects of the nitrogen substituents is currently underway in our group; results will be published shortly.

Acknowledgements

Birkbeck University of London is acknowledged for a studentship (J. S. N.), and we are grateful to Johnson-Matthey for the loan of platinum. Drs G. Steadman (University of Wales, Swansea) and P. King (Birkbeck) are acknowledged for helpful discussions.

References

1 A. L. Lehninger, D. L. Nelson and M. M. Cox, *Principles of Biochemistry*, Worth, New York, 1993.
2 K. B. Wiberg and K. E. Laidig, *J. Am. Chem. Soc.*, 1987, **109**, 5935.
3 K. B. Wiberg and C. M. Breneman, *J. Am. Chem. Soc.*, 1992, **144**, 831.
4 L. M. Cameron and K. E. Laidig, *Can. J. Chem.*, 1993, **71**, 872.
5 K. B. Wiberg and P. R. Rablen, *J. Am. Chem. Soc.*, 1995, **117**, 2201.
6 K. E. Laidig and L. M. Cameron, *J. Am. Chem. Soc.*, 1996, **118**, 1737.

7 L. Pauling, *The Nature of the Chemical bond*, Cornell University Press, Cornell, 1960.
8 J. Sandström, *J. Phys. Chem.*, 1967, **71**, 2318.
9 R. C. Neuman, Jr. and L. B. Young, *J. Phys. Chem.*, 1965, **69**, 2570.
10 A. Loewenstein, R. Melera, P. Rigny and W. Walter, *J. Phys. Chem.*, 1964, **68**, 1597.
11 W. E. Stewart and T. H. Siddall III, *Chem. Rev.*, 1970, **70**, 517.
12 B. J. McCormick, R. Bereman and D. Baird, *Coord. Chem. Rev.*, 1984, **54**, 99.
13 R. F. W. Bader, *Atoms in molecules: a quantum theory*, Oxford University Press, Oxford, 1990.
14 R. F. W. Bader, J. R. Cheeseman, K. E. Laidig, K. B. Wiberg and C. Breneman, *J. Am. Chem. Soc.*, 1990, **112**, 6530.
15 C. J. Perrin, *J. Am. Chem. Soc.*, 1991, **113**, 2865.
16 A. D. Bain, P. Hazendonk and P. Couture, *Can. J. Chem.*, 1999, **77**, 1340.
17 F. Ullman, *Encyclopedia of Industrial Chemistry*, 5th edn., Wiley, New York, 1985, vol. A9, p. 1.
18 M. Motevalli, P. O'Brien, J. R. Walsh and I. M. Watson, *Polyhedron*, 1996, **15**, 2801.
19 R. Argazzi, C. A. Bignozzi, G. M. Hasselman and G. J. Meyer, *Inorg. Chem.*, 1998, **37**, 4533.
20 R. C. Fay, *Coord. Chem. Rev.*, 1996, **154**, 99.
21 E. W. Abel, P. J. Heard, K. Kite, K. G. Orrell and A. F. Psaila, *J. Chem. Soc.*, *Dalton Trans.*, 1996, 1233.
22 D. S. Stephenson and G. Binsch, DNMR 5, Quantum Chemistry Program Exchange, Indian University.
23 E. W. Abel, T. P. J. Coston, K. G. Orrell, V. Šik and D. Stephenson, *J. Magn. Reson.*, 1986, **70**, 34.
24 R. K. Harris, *Nuclear Magnetic Resonance Spectroscopy*, Wiley, New York, 1986.
25 A. D. Bain, T1CALS, McMaster University, 1995.
26 H. Geen and R. Freeman, *J. Magn. Reson.*, 1991, **93**, 93.
27 A. D. Bain and J. A. Cramer, *J. Magn. Reson.*, 1996, **74**, 819.
28 G. Binsch and H. Kessler, *Angew. Chem.*, *Int. Ed. Engl.*, 1980, **19**, 411.
29 G. M. Sheldrick, SHELXL 93, University of Göttingen, 1993.
30 K. Nakamoto, J. Fujita, R. A. Condrate and Y. Morimoto, *J. Chem. Phys.*, 1963, **39**, 423.
31 F. A. Cotton and G. Wilkinson, *Advanced Inorganic Chemistry*, 5th edn., Wiley, New York, 1995.
32 R. B. King (Editor), *Encyclopaedia of Inorganic Chemistry*, Wiley, New York, 1994, vol. 5, p. 2581.
33 A. C. Hazell and M. R. Truter, *Chem. Ind.* (*London*), 1959, 564.
34 A. C. Hazell and M. R. Truter, *Proc. R. Soc. London*, *Ser. A*, 1960, **252**, 218.
35 A. G. Swallow and M. R. Truter, *Proc. R. Soc. London*, *Ser. A*, 1960, **252**, 205.
36 R. N. Hargreaves and M. R. Truter, *J. Chem. Soc. A*, 1969, 2282.
37 C. L. Perrin and T. J. Dwyer, *Chem. Rev.*, 1990, **90**, 935.
38 A. D. Bain and J. A. Cramer, *J. Phys. Chem.*, 1993, **97**, 2884.
39 A. D. Bain and J. A. Cramer, *J. Magn. Reson.*, 1993, **103A**, 217.
40 S. Forsen and R. A. Hoffman, *J. Phys. Chem.*, 1963, **39**, 2892.
41 R. E. Hoffman and S. Forsen, *Prog. Nucl. Magn. Reson. Spectrosc.*, 1966, **1**, 15.
42 R. K. Harris and B. E. Mann, *NMR and the Periodic Table*, Academic Press, London, 1978.
43 P. S. Pregosin, *Ann. Rep. N.M.R. Spectrosc.*, 1986, **17**, 285.
44 K. B. Wiberg, P. R. Rablen, D. J. Rush and T. A. Keith, *J. Am. Chem. Soc.*, 1995, **117**, 4261.
45 P. R. Rablen, D. A. Miller, V. R. Bullock, P. H. Hutchinson and J. A. Gorman, *J. Am. Chem. Soc.*, 1999, **121**, 218.
46 P. R. Rablen, S. A. Pearlman and D. A. Miller, *J. Am. Chem. Soc.*, 1999, **121**, 227.
47 K. G. Orrell, A. G. Osborne, J. O. Prince, V. Šik and D. K. Vellianitis, *Eur. J. Inorg. Chem.*, 2000, 383.
48 U. Haeberlen, *Adv. Magn. Reson. (suppl. 1)*, 1976.